Title	Fast and Simple Construction of Efficient Solar-Water-Splitting Electrodes with Micrometer-Sized Light-Absorbing Precursor Particles
Author(s)	Feng, Jianyong; Zhao, Xin; Ma, Su Su Khine; Wang, Danping; Chen, Zhong; Huang, Yizhong
Citation	Feng, J., Zhao, X., Ma, S. S. K., Wang, D., Chen, Z., & Huang, Y. (2016). Fast and Simple Construction of Efficient Solar-Water-Splitting Electrodes with Micrometer -Sized Light-Absorbing Precursor Particles. Advanced Materials Technologies,1(8), 1600119-.
Date	2016
URL	http://hdl.handle.net/10220/42411
Rights	© 2016 WILEY-VCH Verlag GmbH & Co. KGaA, Weinheim. This is the author created version of a work that has been peer reviewed and accepted for publication by Advanced Materials Technologies, WILEY-VCH Verlag GmbH & Co. KGaA, Weinheim. It incorporates referee's comments but changes resulting from the publishing process, such as copyediting, structural formatting, may not be reflected in this document. The published version is available at: [http://dx.doi.org/10.1002/admt.201600119].

DOI: 10.1002/ ((please add manuscript number))
Article type: Full Paper

Fast and Simple Construction of Efficient Solar-Water-Splitting Electrodes with Micrometer-Sized Light-Absorbing Precursor Particles

*Jianyong Feng, Xin Zhao, Su Su Khine Ma, Danping Wang, Zhong Chen, and Yizhong Huang**

Dr. J. Feng, Dr. X. Zhao, Dr. D. Wang, Prof. Z. Chen, Prof. Y. Huang
School of Materials Science and Engineering
Nanyang Technological University
50 Nanyang Avenue, 639798, Singapore
E-mail: yzhuang@ntu.edu.sg
Dr. S. Ma
Energy Research Institute @ Nanyang Technological University
50 Nanyang Drive, 637553, Singapore

Keywords: solar water splitting, tungsten oxide, bismuth vanadate, cadmium selenide, drop-casting

Micrometer-sized light-absorbing semiconductor particles (usually prepared by high temperature synthetic techniques) hold the desirable merits of high crystallinity, low concentrations of bulk defects and a decreased grain boundary density to reduce bulk recombination of photocarriers. However, solar-water-splitting electrodes assembled using them as precursors always produce very low photocurrents. This could be due to the lack of an effective fabrication and/or modification protocol applicable to assemble these micrometer-sized semiconductor particles into suitable electrode configurations. A fast and simple fabrication scheme of drop-casting followed by the necking treatment is developed to enable the micrometer-sized precursor particles derived photoelectrodes to deliver appreciable photocurrent densities (> 1 mA cm^{-2}). By applying this fabrication scheme, photoelectrodes of solid-state reaction derived Mo doped $BiVO_4$ (ca. 4 μm, modified with oxygen evolution catalysts) and commercial WO_3 (size ranging from 100 nm to > 10 μm) have yielded photocurrent densities higher than 1 mA cm^{-2}, while the photoelectrode composed of commercial CdSe (ca. 10 μm) is able to produce a photocurrent density higher than 5 mA cm^{-2} (in a Na_2S aqueous solution). This strategy provides a new possible way, in addition to

the predominant route of nanostructuring, to construct efficient solar-water-splitting electrodes.

1. Introduction

The efficient and inexpensive production of storable and transportable hydrogen by photoelectrochemical (PEC) water splitting, using the largest renewable source of the sun, is a promising way to achieve a fully sustainable global energy economy.[1] Nanostructuring of the water-splitting photoelectrodes can shorten the migration length for minority carriers, increase the volume ratio of space charge region to photoelectrode bulk and enlarge specific surface area simultaneously, by which continuous and appreciable performance improvements on these solar-water-splitting electrodes have been achieved.[2] This strategy, nanostructuring of photoelectrodes, has therefore been a prevailing trend and a top priority over other approaches to the development of high-efficiency solar-water-splitting electrodes.[3] In some thin film photovoltaic cells (such as lead halide perovskite, copper indium gallium selenide and copper zinc tin sulfide),[4] as well as some p-type photocathodes for water reduction (examples including copper gallium selenide, copper indium gallium selenide and copper zinc tin sulfide, their electrode structures are intrinsically identical with their photovoltaic cell counterparts),[5] however, producing continuous, smooth films with micrometer-sized grains has been proved to be a strong strategy to dramatically improve their overall solar-energy conversion efficiencies.

The above two seemingly contrary material design concepts for light absorbers, however, point to the same goal of improving charge transport and separation in material bulk, i.e. reducing bulk recombination.[2] This can be rationalized by the effective transfer distances for photogenerated charge carriers (electrons and holes), which are the sum of the width of space charge region and charge carrier diffusion lengths.[1d] In the space charge region, charge carriers transport by drift, thereby the recombination within this region is negligible; in the

quasi-neutral region of the light absorber (where bulk recombination occurs), charge carriers transport by diffusion, which is largely influenced by material crystallinity and bulk defects that can affect carrier mobilities and lifetimes. Nanostructuring of photoelectrodes to reduce bulk recombination takes advantage of increasing the contribution of charge drift to the effective transfer distances of charge carriers, by increasing the volume ratio of space charge region to photoelectrode bulk.[6] As discussed above, upon nanostructuring of photoelectrodes, the required migration length for minority carriers is also reduced to match with their effective transfer distance. These two unique features rendered by the nanostructuring strategy provide the possibility and means to reduce bulk recombination in PEC water splitting cells. In comparison, the formation of highly crystalline and large-grained films can minimize the grain boundary density and the concentrations of other bulk defects that induce electron-hole recombination, leading to greatly prolonged charge carrier diffusion lengths.[7] Therefore, the strategy of forming highly crystalline and large-grained films represents a straightforward way to reduce bulk recombination, by addressing the fundamental issue of slow/poor carrier transport in these light-absorbing materials.

To date, aimed at obtaining high-efficiency solar-water-splitting electrodes, much attention has been paid to the nanostructuring strategy;[8] the electrodes that are assembled with micrometer-sized light-absorbing precursor particles usually show sluggish activity therefore receive little attention. Similar to lead halide perovskite and Cu-based thin film photovoltaic materials, these micrometer-sized light-absorbing particles (usually prepared by the solid-state reaction, or other high temperature synthetic techniques) exhibit favorable characteristics of high crystallinity, low concentrations of bulk defects and a decreased grain boundary density to reduce bulk recombination. As such, engineering their potentials as solar-water-splitting electrodes to produce appreciable photocurrent densities (> 1 mA cm^{-2}) is theoretically achievable. However, it remains a major challenge to reach this goal, possibly due to the lack of an effective fabrication and/or modification protocol applicable to assemble

these micrometer-sized light-absorbing precursor particles into suitable electrode configurations. In the present study, we address this challenge by introducing a drop-casting method followed by the necking treatment to enable this type of solar-water-splitting electrodes constructed by micrometer-sized light-absorbing precursor particles to deliver appreciable photocurrent densities (> 1 mA cm^{-2}). By applying this fabrication scheme, photoelectrodes of solid-state reaction derived Mo doped $BiVO_4$ (with an average particle size of ca. 4 μm, modified with oxygen evolution catalysts) and commercial WO_3 (with a large particle size distribution from 100 nm to > 10 μm) have demonstrated photocurrent densities higher than 1 mA cm^{-2}, while the photoelectrode composed of commercial CdSe (with an average particle size of ca. 10 μm) is able to produce a photocurrent density higher than 5 mA cm^{-2} (in a Na_2S aqueous solution). Our study therefore affords a simple but effective route to construct efficient solar-water-splitting electrodes using micrometer-sized light-absorbing precursor particles.

2. Results and Discussion

A solid-state reaction was used to prepare Mo doped micrometer-sized $BiVO_4$ particles (designated as Mo:$BiVO_4$, with 3 atom% Mo at V sites).[9] The X-ray diffraction analysis reveals that the Mo:$BiVO_4$ sample possesses a monoclinic scheelite structure, with a direct band gap of ~ 2.4 eV (Figure S1 and S2, Supporting Information). After grinding, Mo:$BiVO_4$ particles were deposited onto fluorine doped tin oxide (FTO) glass substrates using a drop-casting method. A post-necking treatment with the ammonium metatungstate methanol solution and annealing in air were conducted to produce the Mo:$BiVO_4$ photoanodes for the PEC water splitting evaluation. **Figure 1** shows the photocurrent-potential curves of Mo:$BiVO_4$ photoanodes (with a loading amount of 2 mg cm^{-2}) measured in a 0.1 M potassium phosphate electrolyte (pH = 7) under AM 1.5 G simulated sunlight (100 mW cm^{-2}). The photocurrent measured is negligibly low (in the range of less than 20 μA cm^{-2} as shown

in Figure S3 in the Supporting Information) on the Mo:$BiVO_4$ photoanode without any necking agent. The photocurrent increases by a factor of 51 to ~ 0.68 mA cm^{-2} at 1.8 V_{RHE} for ammonium metatungstate and WCl_6 treated Mo:$BiVO_4$ photoanodes compared with the necking-agent-free one, suggesting the importance of forming effective connections between the light-absorbing particles and the FTO substrate. TiO_2 (formed from titanium (IV) bis(ammonium lactato) dihydroxide upon calcination) can also be used to link the isolated Mo:$BiVO_4$ particles with the FTO substrate. It brings about an increase by a factor of 7.5 in the photocurrent at 1.8 V_{RHE} (~ 110 μA cm^{-2}), far lower than ammonium metatungstate and WCl_6 do. This is due to the slightly higher conduction band edge of TiO_2 than that of $BiVO_4$, which prohibits the efficient electron collection by the FTO substrate from Mo:$BiVO_4$ via the TiO_2 bridge; while for ammonium metatungstate and WCl_6 treated Mo:$BiVO_4$ photoanodes, a favorable band alignment to assist charge separation can be formed between WO_3 and $BiVO_4$.[10]

Although the WCl_6 treated Mo:$BiVO_4$ photoanode performs better at lower applied potentials than the one treated by ammonium metatungstate, it shows a clear color change from bright yellow to dark yellow upon the WCl_6 treatment. This is likely due to the reactions of Mo:$BiVO_4$ with HCl produced during the dissolution of WCl_6 in methanol. Although the final heat treatment can transform the reaction products between HCl and Mo:$BiVO_4$ back to Mo:$BiVO_4$, the morphology change of the Mo:$BiVO_4$ photoanode is inevitable. This hypothesis is supported by the scanning electron microscopy (SEM) observation as shown in **Figure 2**, an abrupt morphology change occurs for the WCl_6 treated Mo:$BiVO_4$ photoanode as compared with the Mo:$BiVO_4$ precursor particles. The Mo:$BiVO_4$ precursor particles as prepared by the solid-state reaction are the aggregates of several oval-like crystalline grains with smooth surfaces, showing an average particle size of ca. 4 μm (see Figure S4 in the Supporting Information). The necking treatment with ammonium metatungstate does not bring about obvious changes on the morphology of Mo:$BiVO_4$ (Figure 2a,b), while a large

amount of pores are produced across the entire surface of the Mo:$BiVO_4$ particles when treated with WCl_6 (Figure 2c). The inter-particle connection and the connection between the FTO substrate and the Mo:$BiVO_4$ particles are important for efficient charge carrier collection, these connections are ensured by the use of the ammonium metatungstate necking agent (Figure S5, Supporting Information). To avoid any unexpected effects brought by the WCl_6 treatment on Mo:$BiVO_4$ photoanodes, ammonium metatungstate treated Mo:$BiVO_4$ photoanodes were chosen for further analyses and modifications. The photocurrent-potential curves of Mo:$BiVO_4$ photoanodes (2 mg cm^{-2}, treated with ammonium metatungstate) are readily reproducible on several repeat samples (more than 20 electrodes from 5 batches of samples, see Figure S6 in the Supporting Information), some of them are shown in **Figure 3**a. Reducing the loading amount of Mo:$BiVO_4$ to 1 mg cm^{-2} gives similar photocurrent-potential responses to Mo:$BiVO_4$ photoanodes of 2 mg cm^{-2}, with a high reproducibility; increasing it to 3 mg cm^{-2} slightly reduces the activity, along with a large sample to sample variation (Figure S7, Supporting Information). In addition, the WO_3 film formed by the ammonium metatungstate alone on the FTO substrate produces a photocurrent density of ~ 60 μA cm^{-2} at 1.8 V_{RHE} (see Figure S8 in the Supporting Information); the annealing temperatures and the amounts of the precursor solution have been optimized to give the best results, increasing the concentration of the ammonium metatungstate methanol solution from 10 mM to 20 mM and 30 mM (while keeping a fixed solution volume used, i.e. 20 μL × 6 for a 2 cm × 1 cm film) results in decreased photocurrent densities (see Figure S9 in the Supporting Information). These results indicate that the observed photocurrents on Mo:$BiVO_4$ photoanodes are mainly produced by Mo:$BiVO_4$, and an excessive application of necking agents leads to a partially covered Mo:$BiVO_4$ surface that blocks the hole transfer process. Surface modifications of Mo:$BiVO_4$ photoanodes with oxygen evolution catalysts (5 mC cm^{-2} of FeO_x, CoO_x and NiO_x), following the procedure developed by a previous report,[11] to improve the surface water oxidation kinetics result in photocurrent densities larger than 1 mA cm^{-2} at 1.7 V_{RHE} for

all cases (Figure 3b). This photocurrent value is already very high considering the reported values of the hole diffusion length (70-200 nm) in $BiVO_4$[12] compared with the average particle size of 4 μm for the present Mo:$BiVO_4$ (the primary particle size for Mo:$BiVO_4$ aggregates is generally ≥ 1 μm). As the width of space charge region is reduced to a few nanometers upon the introduction of the donor dopant of Mo, the contribution of charge diffusion to the effective transfer distances of charge carriers is therefore significant (i.e. large charge carrier diffusion lengths), consistent with the high-crystalline and less-defective nature of the solid-state reaction derived $BiVO_4$ samples. In addition, although the Mo doped $BiVO_4$ photoanode produces a significantly higher photocurrent than its pure counterpart (see Figure S10 in the Supporting Information), the back-side illumination yields a much higher photocurrent than the front-side illumination on the Mo:$BiVO_4$ photoanode, suggesting poor electron transport within this film (see Figure S11 in the Supporting Information).[13] Therefore, further optimization of the synthetic parameters (calcination temperatures, precursors) and the dopant concentration may afford a much higher photocurrent on Mo:$BiVO_4$ photoanodes.[14]

To further confirm the effectiveness of our strategy, commercial CdSe with an average particle size of ca. 10 μm was chosen to construct the corresponding photoelectrode (see Figure S12 in the Supporting Information). A loading amount of 4 mg cm^{-2} was achieved using multiple drop-casting procedures, following which a post-necking treatment with a methanol solution of titanium (IV) bis(ammonium lactato) dihydroxide (10 mM based on Ti) and annealing in N_2 were conducted to produce the CdSe photoanodes. The crystal structure, optical absorption and band gap of the CdSe film are shown in Figure S13 and S14 in the Supporting Information. **Figure 4**a shows the photocurrent-potential curves of CdSe photoanodes measured in a 0.2 M Na_2S aqueous solution (pH = 13) under AM 1.5 G simulated sunlight (100 mW cm^{-2}). CdSe particles alone on FTO glass without the use of necking agents generate a photocurrent density of 1.1 mA cm^{-2} at 0.8 V_{RHE}. Upon the

application of $TiCl_4$, a largely increased photocurrent of 3.2 mA cm^{-2} at 0.8 V_{RHE} is obtained and an even higher photocurrent of 5.2 mA cm^{-2} at 0.8 V_{RHE} is realized when titanium (IV) bis(ammonium lactato) dihydroxide is used as the necking agent.[15] Although the distribution of CdSe particles on FTO is seen to be quite uneven (due to the extremely large particle size), three different photoelectrodes from two batches of samples exhibit quite similar photocurrent-potential curves (Figure 4b), indicating a high reproducibility. For comparison, the TiO_2 film formed by the titanium (IV) bis(ammonium lactato) dihydroxide alone on the FTO substrate shows almost no photoresponse (see Figure S15 in the Supporting Information). The slightly lower photocurrent produced from the $TiCl_4$ treated CdSe photoanode than the one treated by titanium (IV) bis(ammonium lactato) dihydroxide could be due to the chemical etching of CdSe surface by the simultaneously formed HCl during the dissolution of $TiCl_4$ in methanol, as supported by the appearance of a large amount of semi-sphere-like particles on CdSe surface (see **Figure 5**).

We have demonstrated in the previous sections that Mo:$BiVO_4$ and CdSe with the average particle sizes of 4 μm and 10 μm, respectively, are able to afford appreciable photocurrents. An additional study has been carried out on commercial WO_3, to prove that our strategy is also applicable to particulate precursors with a large size distribution. The crystal structure, optical absorption and band gap of the WO_3 film can be found in Figure S16 and S17 in the Supporting Information. The primary particle size of the commercial WO_3 ranges from ca. 100 nm to ca. 1 μm, these particles either loosely aggregate or sinter together firmly to form secondary particles can be as large as > 10 μm (see **Figure 6**a,b and Figure S18 in the Supporting Information). The resulting WO_3 films (with a particle loading amount of 3 mg cm^{-2} and treated with ammonium metatungstate) exhibit a high surface roughness, as that of CdSe films in the present study, they still show a saturation photocurrent of ca. 1.1 mA cm^{-2} and a small film-to-film variation (Figure 6c,d). This photocurrent value is comparable with that of well optimized WO_3 photoanodes (with crystallites of ~ 50 nm in size) prepared by

cathodic electrodeposition from peroxytungstic acid solutions.[16] In addition, the WO_3 film formed by the ammonium metatungstate alone on the FTO substrate produces a photocurrent density of ~ 40 μA cm^{-2} at 1.7 V_{RHE}, indicating a minor contribution to the overall photocurrent on the final WO_3 photoanode (see Figure S19 in the Supporting Information). Reducing or increasing the particle loading amount leads to reduced repeatability (see Figure S20 in the Supporting Information). It is not clear why the WCl_6 treated WO_3 photoanode is less efficient than the one treated by ammonium metatungstate (8.6 times increase versus 2.3 times increase in photocurrent at 1.8 V_{RHE} compared with the necking-agent-free WO_3 photoelectrode), as there is no obvious difference between them two as shown in Figure S18 (Supporting Information); meanwhile, it is also widely accepted WO_3 is resistant to chemical corrosion towards HCl.[17] Combined with the above photocurrent-potential measurements and the SEM analyses performed on Mo:$BiVO_4$ and CdSe photoanodes, great care should be given to the selection of necking agents to form effective connections between the light-absorbing particles and the FTO substrate, which ensure desirable PEC water splitting performances.

Up to now, we have shown the effectiveness of a rather simple and fast fabrication scheme to enable micrometer-sized precursor particles derived photoelectrodes (Mo:$BiVO_4$, CdSe and WO_3) to deliver photocurrent densities larger than 1 mA cm^{-2}. This drop-casting method followed by the necking treatment is further compared with other methods suitable for preparing photoelectrodes using particulate precursors. The first one is the electrophoretic deposition process, which has been a popular method to deal with particulate precursors.[18,19] Unfortunately, we cannot obtain a suspension of Mo:$BiVO_4$ stable enough to perform the electrophoretic deposition (as well as commercial WO_3 and CdSe investigated in this study), as these large particles settle down quickly from the particle suspension. The second technique developed recently called the particle transfer method could in principle be applied to construct electrodes with micrometer-sized precursor particles. However, it is not cost-

effective and involves laborous multi-step processes;[20] meanwhile, it requires metals to form the conducting substrates, under highly crossive and oxidative environmental conditions (as is usually the case with water splitting) side reactions from these metals could be significant. The third method is the doctor blade technique, it needs the addition of organic binders, which may impede the charge transport within the electrodes,[21] to form a paste. These organic binders can only be eliminated through high temperature calcinations in air; however, the high temperature annealing in air basically leads to disastrous damages on non-oxide based semiconductors (for example metal sulfides and metal nitrides). In contrast, the approach we adopt in the present study is a binder-free process, the organic solvents used (methanol and isopropanol) can be easily removed by evaporation at room temperature, making it a suitable strategy to handle almost all kinds of micrometer-sized particulate semiconductors (for example CdSe in the present study). Therefore, the proposed approach here harbors great advantages over other methods for the construction of solar-water-splitting electrodes using micrometer-sized precursor particles.

3. Conclusion

Micrometer-sized light-absorbing semiconductor particles (usually prepared by high temperature synthetic techniques) possess the desirable characteristics of high crystallinity, low concentrations of bulk defects and a decreased grain boundary density to reduce bulk recombination of photocarriers. However, prior to this study, the solar-water-splitting electrodes assembled with these precursor particles are always inefficient therefore attract little attention. We address this problem in this paper by developing a fast and simple fabrication scheme of drop-casting followed by the necking treatment to enable the micrometer-sized precursor particles derived photoelectrodes to deliver appreciable photocurrent densities. Utilizing this strategy, photoelectrodes of Mo doped $BiVO_4$ with an average particle size of ca. 4 μm (modified with oxygen evolution catalysts), and commercial

WO_3 with a large particle size distribution from 100 nm to > 10 μm, have demonstrated photocurrent densities higher than 1 mA cm^{-2}; the photoelectrode composed of commercial CdSe with an average particle size of ca. 10 μm is able to afford a photocurrent density higher than 5 mA cm^{-2} (in a Na_2S solution), demonstrating the effectiveness of the present strategy. Additionally, we emphasize the necessity of forming effective connections between the light-absorbing particles and the FTO substrate, and the importance of selecting suitable necking agents, to guarantee high performance in these particulate photoelectrodes. As such, the photocurrent increases by a factor of 51 at 1.8 V_{RHE} for ammonium metatungstate and WCl_6 treated Mo:$BiVO_4$ photoanodes compared with the necking-agent-free one, and using titanium (IV) bis(ammonium lactato) dihydroxide as the necking agent brings about an increase by a factor of 7.5. For CdSe photoelectrodes, titanium (IV) bis(ammonium lactato) dihydroxide performs much better than $TiCl_4$ when used as the necking agent (3.7 times increase versus 1.9 times increase in photocurrent at 0.8 V_{RHE} compared with the necking-agent-free CdSe photoelectrode). While for WO_3 photoelectrodes, ammonium metatungstate and WCl_6 treated photoelectrodes produce 8.6 times and 2.3 times higher photocurrents at 1.8 V_{RHE} than the necking-agent-free WO_3 photoelectrode, respectively. Depositing an underlayer/blocking layer (before the drop-casting process) as usually adopted in TiO_2-based dye-sensitized solar cells to reduce the back reduction of photo-oxidized products on the unlapped FTO substrate will further improve the PEC performances of the present discontinuous photoanode films.[22] Our strategy allows a logical extension to other micrometer-sized light-absorbing semiconductor (including p-type semiconductors) particles that are commercially available or obtained by high temperature synthetic techniques, thus providing a new possible way, in addition to the predominant route of nanostructuring, to fabricate high-efficiency solar-water-splitting electrodes.

4. Experimental Section

Preparation of Mo doped $BiVO_4$ Particles: Mo doped micrometer-sized $BiVO_4$ particles (3 atom% Mo at V sites, or $BiV_{0.97}Mo_{0.03}O_4$) were prepared by a previously reported solid-state reaction process. Specifically, stoichiometric amount of Bi_2O_3, V_2O_5 and MoO_3 were mixed and ground in an agate mortar, with appropriate amount of ethanol. The mixture was then heated at 600 ℃ for 2 h and 800 ℃ for 3 h, respectively, with intermediate grinding.

Fabrication of Photoanode Films: All the photoanode films in the present study were fabricated using a drop-casting method followed by the necking treatment. Taking Mo:$BiVO_4$ as an example, 20 mg of Mo:$BiVO_4$ powder (finely ground) was dispersed in 500 μL isopropanol with the assistance of sonication to obtain a uniform powder suspension. The drop-casting process was conducted by dropping 50 μL suspension onto a 2 cm × 1 cm FTO glass substrate. After drying in air, the next drop-casting process was applied to get a desired loading amount of 2 mg cm^{-2} for Mo:$BiVO_4$. The Mo:$BiVO_4$ electrodes (2 cm × 1 cm) were dropped with the ammonium metatungstate methanol solution (10 mM based on W, 20 μL) then dried in air. Note that ammonium metatungstate hydrate is not soluble in methanol, the desired amount of ammonium metatungstate hydrate was firstly dissolved completely in 0.2 mL DI water, following which methanol was added to form a 10 mL methanol solution with the concentration of solute at 10 mM based on W. This procedure was repeated for six times. Finally, the dropped Mo:$BiVO_4$ electrodes were scrubbed with a piece of paper to leave a coating area of ca. 1 cm × 1 cm and heated at 500 ℃ for 1 h in air. Similar procedures were adopted for commercial WO_3 (Sigma-Aldrich, ≤20 μm) and CdSe (Sigma-Aldrich, ca. 10 μm) particles, with CdSe photoanode films being heated at 400 ℃ for 2 h under a flow of N_2 (flow rate: 50 mL min^{-1}).

Photoelectrochemical Characterization: Photoelectrochemical measurements were carried out in a three-electrode configuration cell, with Mo:$BiVO_4$, WO_3 and CdSe films as the working electrodes, Ag/AgCl in saturated KCl as the reference electrode, and Pt foil as the counter electrode. For electrolytes, a 0.1 M potassium phosphate aqueous solution (pH = 7) was used

for Mo:$BiVO_4$, a 0.33 M H_3PO_4 aqueous solution (pH = 1.28) was used for WO_3, and a 0.2 M Na_2S aqueous solution (pH = 13) were used for CdSe. Potentials are reported vs. reversible hydrogen electrode (RHE). Photocurrent densities were recorded under AM 1.5 G simulated sunlight (100 mW cm^{-2}), from an Asahi HAL-320 EX3 simulator. The light intensity of the sunlight simulator was calibrated at 100 mW cm^{-2} by the standard reference of a Newport 91150V silicon cell before use. The irradiated area was a circle with a diameter of ca. 6 mm.

Sample Characterization: The crystal structures of all the samples were measured by thin film X-ray diffraction (XRD, Shimadzu LabX-XRD-6000) with Cu Kα radiation (λ = 1.5418 Å). The optical absorption spectra of the thin film samples were obtained on an UV-visible-near-infrared (UV-Vis-NIR) spectrophotometer (PerkinElmer, Lambda 750 UV/Vis/NIR spectrophotometer). The morphology of the thin film samples was observed by field-emission scanning electron microscopy (FE-SEM; JEOL, JSM-7600F), and no conductive coating was deposited onto samples for these SEM measurements.

Supporting Information

Supporting Information is available from the Wiley Online Library or from the author.

Acknowledgements

J. Feng and X. Zhao contributed equally to this work. This research was support by SUG (Start-up funding in NTU), Tier 1 (AcRF grant MOE Singapore M401992), Tier 2 (AcRF grant MOE Singapore M4020159), Chinese Natural Science Foundation (Grant 51271031 and 50701006) and National Basic Research Program (No. 2014CB6433000)

Received: ((will be filled in by the editorial staff))
Revised: ((will be filled in by the editorial staff))
Published online: ((will be filled in by the editorial staff))

[1] a) M. Grätzel, *Nature* **2001**, *414*, 338; b) N. S. Lewis, D. G. Nocera, *Proc. Natl. Acad. Sci. U.S.A.* **2006**, *103*, 15729; c) O. Khaselev, J. A. Turner, *Science* **1998**, *280*, 425; d) Z. Li, W. Luo, M. Zhang, J. Feng, Z. Zou, *Energy Environ. Sci.* **2013**, *6*, 347.

[2] Z. Li, J. Feng, S. Yan, Z. Zou, *Nano Today* **2015**, *10*, 468.

[3] a) S. D. Tilley, M. Cornuz, K. Sivula, M. Grätzel, *Angew. Chem. Int. Ed.* **2010**, *49*, 64058; b) J. Brillet, M. Grätzel, K. Sivula, *Nano Lett.* **2010**, *10*, 4155; c) B. D. Alexander, P. J. Kulesza, L. Rutkowska, R. Solarska, J. Augustynski, *J. Mater. Chem.* **2008**, *18*, 2298; d) W. Luo, Z. Yang, Z. Li, J. Zhang, J. Liu, Z. Zhao, Z. Wang, S. Yan, T. Yu, Z. Zou, *Energy Environ. Sci.* **2011**, *4*, 4046.

[4] a) A. Sharenko, M. F. Toney, *J. Am. Chem. Soc.* **2016**, *138*, 463; b) S. Ishizuka, A. Yamada, H. Shibata, P. Fons, K. Sakurai, K. Matsubara, S. Niki, *Sol. Energy Mater. Sol. Cells* **2009**, *93*, 792; c) S. Ahmed, K. B. Reuter, O. Gunawan, L. Guo, L. T. Romankiw, H. Deligianni, *Adv. Energy Mater.* **2012**, *2*, 253.

[5] a) B. Marsen, B. Cole, E. L. Miller, *Sol. Energy Mater. Sol. Cells* **2008**, *92*, 1054; b) F. Jiang, Gunawan, T. Harada, Y. Kuang, T. Minegishi, K. Domen, S. Ikeda, *J. Am. Chem. Soc.* **2015**, *137*, 13691; c) Z. Guan, W. Luo, J. Feng, Q. Tao, Y. Xu, X. Wen, G. Fu, Z. Zou, *J. Mater. Chem. A.* **2015**, *3*, 7840.

[6] a) X. Zhao, W. Luo, J. Feng, M. Li, Z. Li, T. Yu, Z. Zou, *Adv. Energy Mater.* **2014**, *4*, 1301785; b) T. Kim, K. Choi, *Science* **2014**, *343*, 990; c) K. Sivula, *J. Phys. Chem. Lett.* **2013**, *4*, 1624.

[7] a) J. Feng, W. Luo, T. Fang, H. Lv, Z. Wang, J. Gao, W. Liu, T. Yu, Z. Li, Z. Zou, *Adv. Funct. Mater.* **2014**, *24*, 3535; b) S. Warren, K. Voïtchovsky, H. Dotan, C. Leroy, M. Cornuz, F. Stellacci, C. Hébert, A. Rothschild,M. Grätzel, *Nat. Mater.* **2013**, *12*, 842.

[8] a) K. Sivula, F. Le Formal, M. Grätzel, *ChemSusChem* **2011**, *4*, 432; b) Y. Lin, G. Yuan, S. Sheehan, S. Zhou, D. Wang, *Energy Environ. Sci.* **2011**, *4*, 4862; c) Y. Ling, G. Wang, J. Reddy, C. Wang, J. Zhang, Y. Li, *Angew. Chem. Int. Ed.* **2012**, *51*, 4074; d) X. Feng,

T. LaTempa, J. Basham, G. Mor, O. Varghese, C. Grimes, *Nano Lett.* **2010**, *10*, 948; e) Y. Sun, H. Cheng, S. Gao, Z. Sun, Q. Liu, Q. Liu, F. Lei, T. Yao, J. He, S. Wei, Y. Xie, *Angew. Chem. Int. Ed.* **2012**, *51*, 8727.

[9] W. Yao, H. Iwai, J. Ye, *Dalton Trans.* **2008**, 1426.

[10] P. Rao, L. Cai, C. Liu, I. Cho, C. Lee, J. Weisse, P. Yang, X. Zheng, *Nano Lett.* **2014**, *14*, 1099.

[11] L. Martinez, D. Leinen, F. Martín, M. Gabas, J. Ramos-Barrado, E. Quagliata, E. Dalchiele, *J. Electrochem. Soc.* **2007**, *154*, D126.

[12] a) D. K. Zhong, S. Choi, D. R. Gamelin, *J. Am. Chem. Soc.* **2011**, *133*, 18370; b) F. Abdi, T. Savenije, M. May, B. Dam, R. van de Krol, *J. Phys. Chem. Lett.* **2013**, *4*, 2752; c) R. Pala, A. Leenheer, M. Lichterman, H. Atwater, N. Lewis, *Energy Environ. Sci.* **2014**, *7*, 3424; d) A. Rettie, H. Lee, L. Marshall, J. Lin, C. Capan, J. Lindemuth, J. McCloy, J. Zhou, A. Bard, C. Mullins, *J. Am. Chem. Soc.* **2013**, *135*, 11389.

[13] a) F. Abdi, R. van de Krol, *J. Phys. Chem. C* **2012**, *116*, 9398; b) Y. Liang, T. Tsubota, L. Mooij, R. van de Krol, *J. Phys. Chem. C* **2011**, *115*, 17594.

[14] a) J. Feng, D. Cao, Z. Wang, W. Luo, J. Wang, Z. Li, Z. Zou, *Chem. - Eur. J.* **2014**, *20*, 16384; b) W. Luo, J. Wang, X. Zhao, Z. Zhao, Z. Li, Z. Zou, *Phys. Chem. Chem. Phys.* **2013**, *15*, 1006.

[15] a) M. Schierhorn, S. Boettcher, S. Kraemer, G. Stucky, M. Moskovits, *Nano Lett.* **2009**, *9*, 3262; b) J. Miao, H. Yang, S. Khoo, B. Liu, *Nanoscale* **2013**, *5*, 11118.

[16] Q. Mi, A. Zhanaidarova, B. Brunschwig, H. Gray, N. Lewis, *Energy Environ. Sci.* **2012**, *5*, 5694.

[17] R. Solarska, R. Jurczakowski, J. Augustynski, *Nanoscale* **2012**, *4*, 1553.

[18] P. Sarkar, P. Nicholson, *J. Am. Ceram. Soc.* **1996**, *79*, 1987.

[19] a) C. Leroy, A. Maegli, K. Sivula, T. Hisatomi, N. Xanthopoulos, E. Otal, S. Yoon, A. Weidenkaff, R. Sanjines, M. Grätzel, *Chem. Commun.* **2012**, *48*, 820; b) M. Liao, J. Feng, W.

Luo, Z. Wang, J. Zhang, Z. Li, T. Yu, Z. Zou, *Adv. Funct. Mater.* **2012**, *22*, 3066; c) M. Higashi, K. Domen, R. Abe, *Energy Environ. Sci.* **2011**, *4*, 4138.

[20] T. Minegishi, N. Nishimura, J. Kubota, K. Domen, *Chem. Sci.* **2013**, *4*, 1120.

[21] X. Lu, C. Zhao, *Nat. Commun.* **2015**, *6*, 6616.

[22] D. Eisenberg, H. Ahn, A. Bard, *J. Am. Chem. Soc.* **2014**, *136*, 14011.

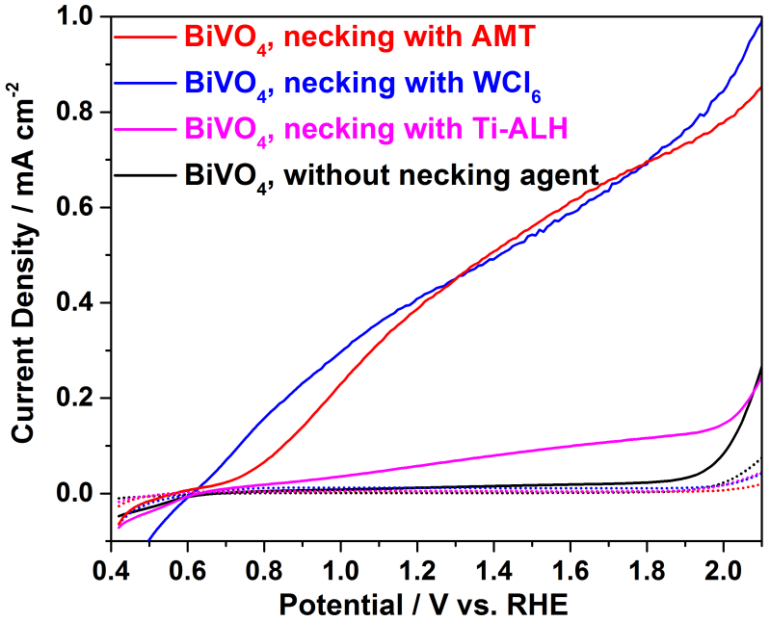

Figure 1. Current-potential curves of Mo:$BiVO_4$ photoanodes (with a loading amount of 2 mg cm^{-2}) treated with different necking agents in the dark (dotted lines) and under simulated solar illumination (solid lines); AMT, ammonium metatungstate, Ti-ALH, titanium (IV) bis(ammonium lactato) dihydroxide. The electrolyte is a 0.1 M potassium phosphate aqueous solution (pH = 7), the scan rate is 30 mV s^{-1}.

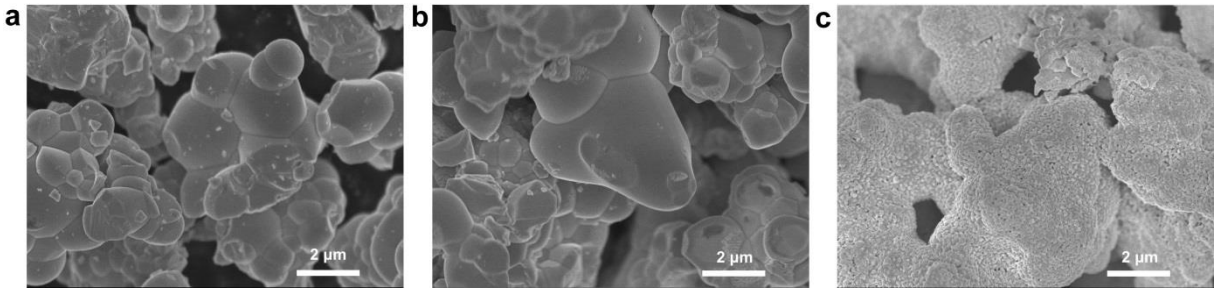

Figure 2. SEM images of (a) Mo:$BiVO_4$ powders, Mo:$BiVO_4$ photoanodes treated with (b) ammonium metatungstate and (c) WCl_6.

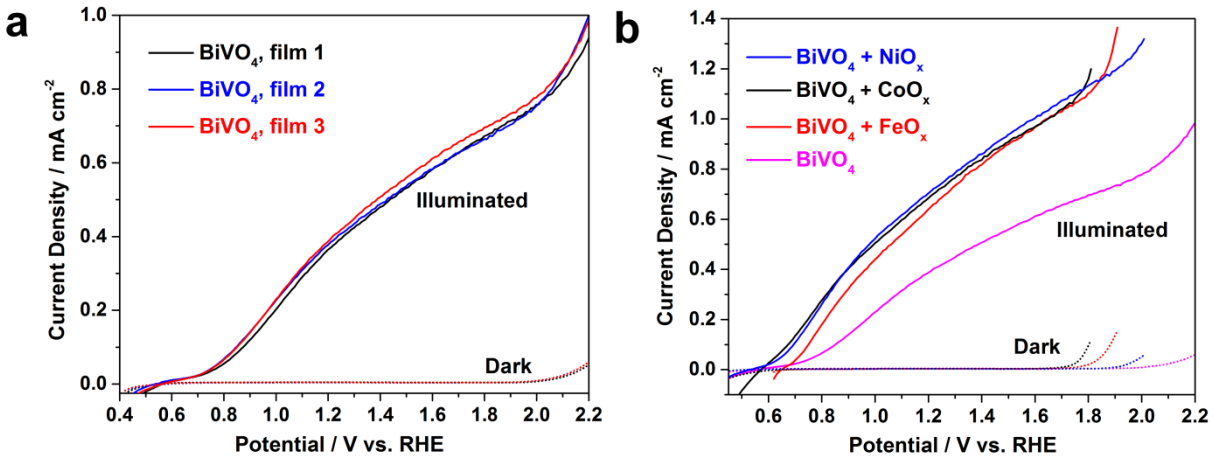

Figure 3. (a) Current-potential curves of Mo:$BiVO_4$ photoanodes (with a loading amount of 2 mg cm^{-2}) treated with ammonium metatungstate in the dark (dotted lines) and under simulated solar illumination (solid lines). (b) Current-potential curves of Mo:$BiVO_4$ photoanodes (with a loading amount of 2 mg cm^{-2} and treated with ammonium metatungstate) modified with oxygen evolution catalysts of FeO_x, CoO_x and NiO_x (5 mC cm^{-2} for all cases) in the dark (dotted lines) and under simulated solar illumination (solid lines). The electrolyte is a 0.1 M potassium phosphate aqueous solution (pH = 7), the scan rate is 30 mV s^{-1}.

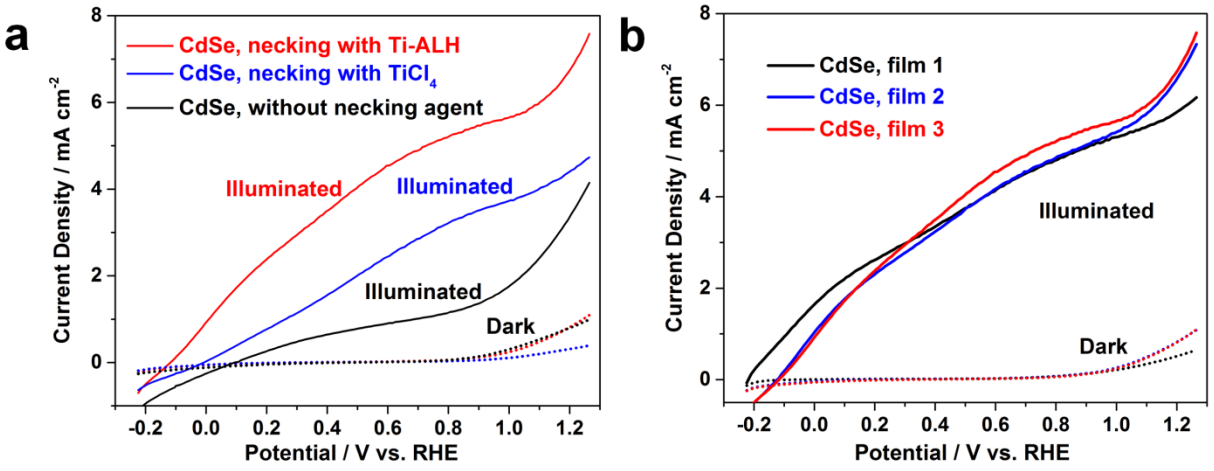

Figure 4. (a) Current-potential curves of CdSe photoanodes (with a loading amount of 4 mg cm^{-2}) treated with different necking agents in the dark (dotted lines) and under simulated solar illumination (solid lines); Ti-ALH, titanium (IV) bis(ammonium lactato) dihydroxide. (b) Current-potential curves of CdSe photoanodes (with a loading amount of 4 mg cm^{-2}) treated with titanium (IV) bis(ammonium lactato) dihydroxide in the dark (dotted lines) and under simulated solar illumination (solid lines). The electrolyte is a 0.2 M Na_2S aqueous solution (pH = 13), the scan rate is 30 mV s^{-1}.

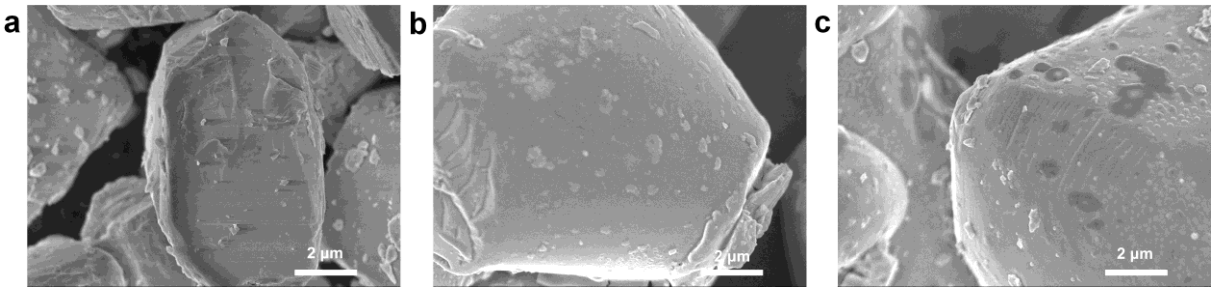

Figure 5. SEM images of (a) CdSe powders, CdSe photoanodes treated with (b) titanium (IV) bis(ammonium lactato) dihydroxide and (c) $TiCl_4$.

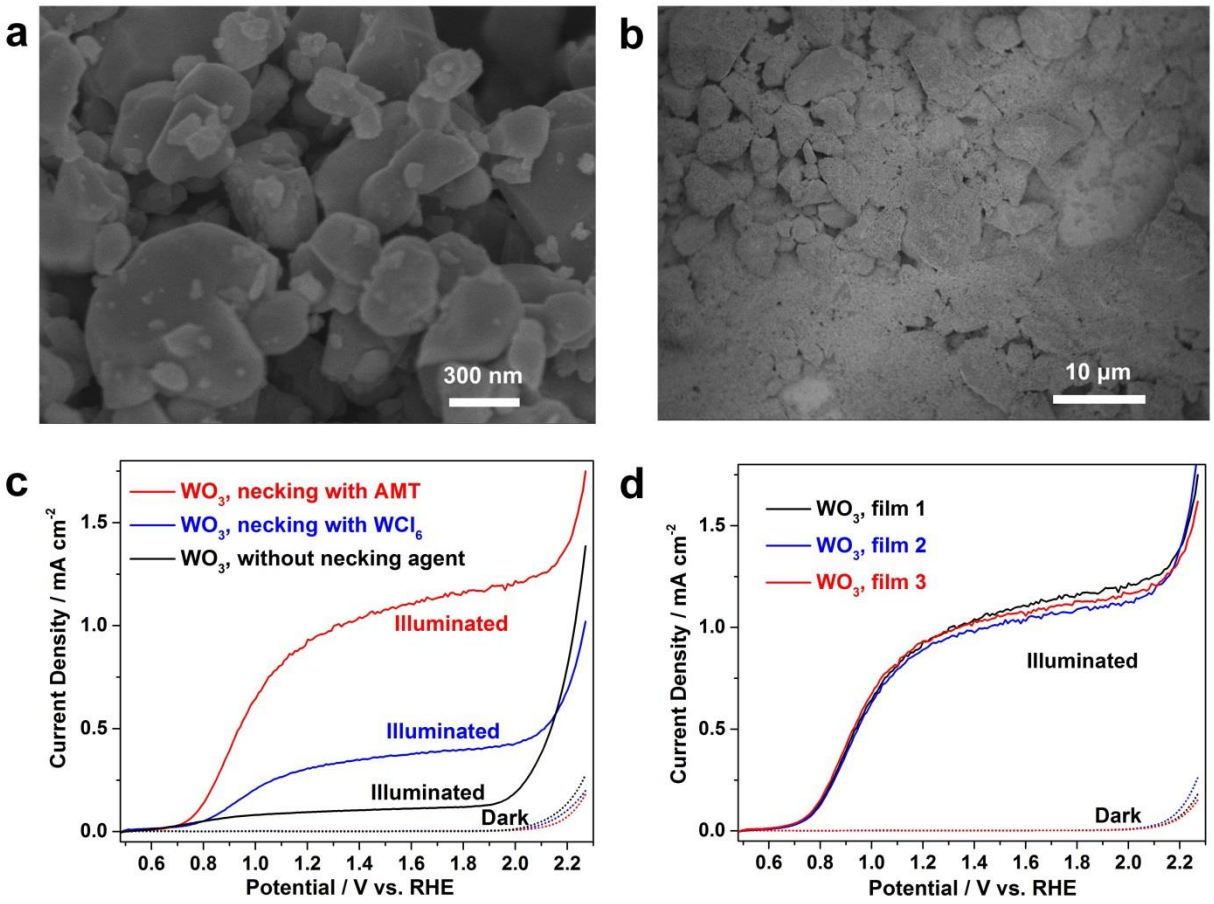

Figure 6. (a) High-magnification and (b) low-magnification SEM images of WO_3. (c) Current-potential curves of WO_3 photoanodes (with a loading amount of 3 mg cm^{-2}) treated with different necking agents in the dark (dotted lines) and under simulated solar illumination (solid lines); AMT, ammonium metatungstate. (d) Current-potential curves of WO_3 photoanodes (with a loading amount of 3 mg cm^{-2}) treated with ammonium metatungstate in the dark (dotted lines) and under simulated solar illumination (solid lines). The electrolyte is a 0.33 M H_3PO_4 aqueous solution (pH = 1.28), the scan rate is 30 mV s^{-1}.

The table of contents entry

A fast and simple fabrication scheme is developed to construct solar-water-splitting electrodes using micrometer-sized light-absorbing semiconductor particles, i.e. solid-state reaction derived Mo doped $BiVO_4$ (ca. 4 μm), commercial WO_3 (particle sizes ranging from 100 nm to > 10 μm) and commercial CdSe (ca. 10 μm). These photoelectrodes are able to deliver appreciable photocurrent densities (> 1 mA cm^{-2}).

Keyword Photocatalysis

J. Y. Feng, X. Zhao, S. S. K. Ma, D. P. Wang, Z. Chen, and Y. Z. Huang*

Fast and Simple Construction of Efficient Solar-Water-Splitting Electrodes with Micrometer-Sized Light-Absorbing Precursor Particles

ToC figure